Spring 4-17-2023

Kinetic Analysis of Glu115Ala Cytosolic Human Malate Dehydrogenase Mutation Shows a Change in Activity on Non-native Substrate Phenylpyruvate

Kailey Paar
Providence College

Kinetic analysis of Glu115Ala cytosolic human malate dehydrogenase mutation shows a change in activity on non-native substrate phenylpyruvate

Submitted for publication, 13 May 2022

Kailey Paar and Kathleen Cornely

Department of Chemistry and Biochemistry, Providence College, Providence, RI, 02918

The cytosolic human enzyme, malate dehydrogenase (MDH1), is believed to have a significant effect on the proliferation of cancerous cells. This enzyme oxidizes NADH to NAD^+ as it converts oxaloacetate (OAA) to malate. This oxidation of NADH provides the needed NAD^+ to cancer cells, which require NAD^+ as they upregulate glycolysis in aerobic conditions. Targeting MDH1 can reveal new therapeutic treatments for cancer by preventing the conversion of OAA to malate and depleting NAD^+ stores in cancer cells, which can be done by mutating residues in the enzyme and assessing the change in activity. Here we show the replacement of a glutamate with an alanine at position 115 (E115A) of MDH1 through site-directed mutagenesis and Ni-NTA protein purification to analyze the change in the enzymatic activity on native and non-native substrates of the enzyme. A modified Michaelis-Menten equation was utilized to determine that the wild-type enzyme has a k_{sp} of $6 \pm 1 \times 10^6$ $M^{-1}s^{-1}$ on OAA and $1.12 \pm 0.05 \times 10^3$ $M^{-1}s^{-1}$ on phenylpyruvate while the E115A mutant enzyme has k_{sp} values of $6.3 \pm 0.5 \times 10^6$ $M^{-1}s^{-1}$ and 400 ± 40 $M^{-1}s^{-1}$ on OAA and phenylpyruvate respectively. The data suggest that the E115A mutation has a higher affinity for OAA, lower affinity for phenylpyruvate, and decreased specificity for phenylpyruvate compared to the wild-type. More research can be conducted to address and manipulate the affinity of MDH1 for a non-native substrate to inhibit the enzyme in cancerous cells.

The Warburg effect describes the characteristic of cancer cells to have increased uptake and metabolism of anaerobic glucose processing in aerobic conditions (1). This increase in glycolysis benefits cancer cells, allowing them to grow and invade, potentially leading to metastasis. This glycolysis is regulated by the need for the regeneration of nicotinamide adenine dinucleotide (NAD^+), which is known to occur when lactate dehydrogenase (LDH, EC: 1.1.1.27) converts pyruvate to lactate. Alternatively, malate dehydrogenase (MDH, EC: 1.1.137) functions in the malate-aspartate shuttle to catalyze the reaction that converts oxaloacetate (OAA) to malate with NADH as a cofactor (1). Human MDH can exist in a cytosolic and mitochondrial form, where the cytosolic form is responsible for the oxidation of NADH to NAD^+ necessary for the function of glycolysis which is important for cancer cells (2). The mitochondrial form is known as hMDH2 (which functions in the citric acid cycle), and the cytosolic form is hMDH1.

Because hMDH1 also regenerates NAD^+, it may be a control point for glycolysis required by cancer cells just as is LDH (1). Therefore, studying the activity of hMDH1

can lead to further insight into its relation to the proliferation of cancer cells. The enzyme contains a mobile loop made up of various residues from position 105 to 123. We hypothesize that changing non-conserved residues on this mobile loop will affect the substrate specificity and binding of the hMDH1 enzyme on its native substrate as well as on a non-native substrate. With this hypothesis, we propose that changing a non-conserved residue on the mobile loop to a smaller, neutral, and hydrophobic residue will lead to a change in the affinity of the enzyme for its native substrate, OAA, and increase affinity for a non-native substrate, phenylpyruvate. Changing the enzyme's affinity for an alternative substrate may lead to new developments of cancer treatment that would target the MDH1 pathway. We proposed that the mutation of glutamate, which is negatively charged and hydrophilic, to an alanine, which is not charged and is hydrophobic, will change the substrate specificity of malate dehydrogenase. Since alanine is also a smaller amino acid than glutamate, we hypothesized that the mutation from glutamate to alanine would allow malate dehydrogenase to accommodate a larger, non-native substrate, phenylpyruvate. Here we present that, through kinetics data, the mutation of glutamate at position 115 to an alanine did not increase the affinity for the non-native substrate, phenylpyruvate as hypothesized. The mutation instead lowered the enzyme's efficiency and specificity for both phenylpyruvate and OAA, and increased affinity for the non-native substrate, OAA.

Results

Determining the mutation

A multiple sequence alignment was conducted by searching UniProt (UniProt ID code: P40925) (3) for malate dehydrogenase in various classes that contained the enzyme in the cytoplasm and then aligning their sequences. Conserved residues were noted as immutable, as mutating these residues would result in inactivation of the enzyme. The mutation was chosen by looking at various PyMOL images displaying the active site and important residues for the activity of the enzyme (4). The hMDH1 enzyme contains asparagine residues at positions 123 and 149 that are responsible for binding NAD^+ as well as residues R110 and R180 that orient the substrate OAA. Another arginine at position 116 stabilizes the transition state. The catalytic dyad is made up of an aspartate at position 177 and histidine at position 205 which are responsible for the enzyme's catalytic activity (Fig. 1). The mutation was limited to the residues contained in the mobile loop, which are residues 105 through 123 and Glu115 was chosen because it is within this mobile loop and is not immutable. It was hypothesized that the mutation of Glu115 to an alanine would lead to many changes that would determine if charge, size, polarity, and hydrophilicity is important for the malate dehydrogenase activity. The smaller size of the alanine residue was also believed to make the enzyme accommodate a larger substrate.

Computational analysis of the mutation

The sequence of the mutated enzyme was uploaded to the program AlphaFold to predict the tertiary structure (5). This prediction was

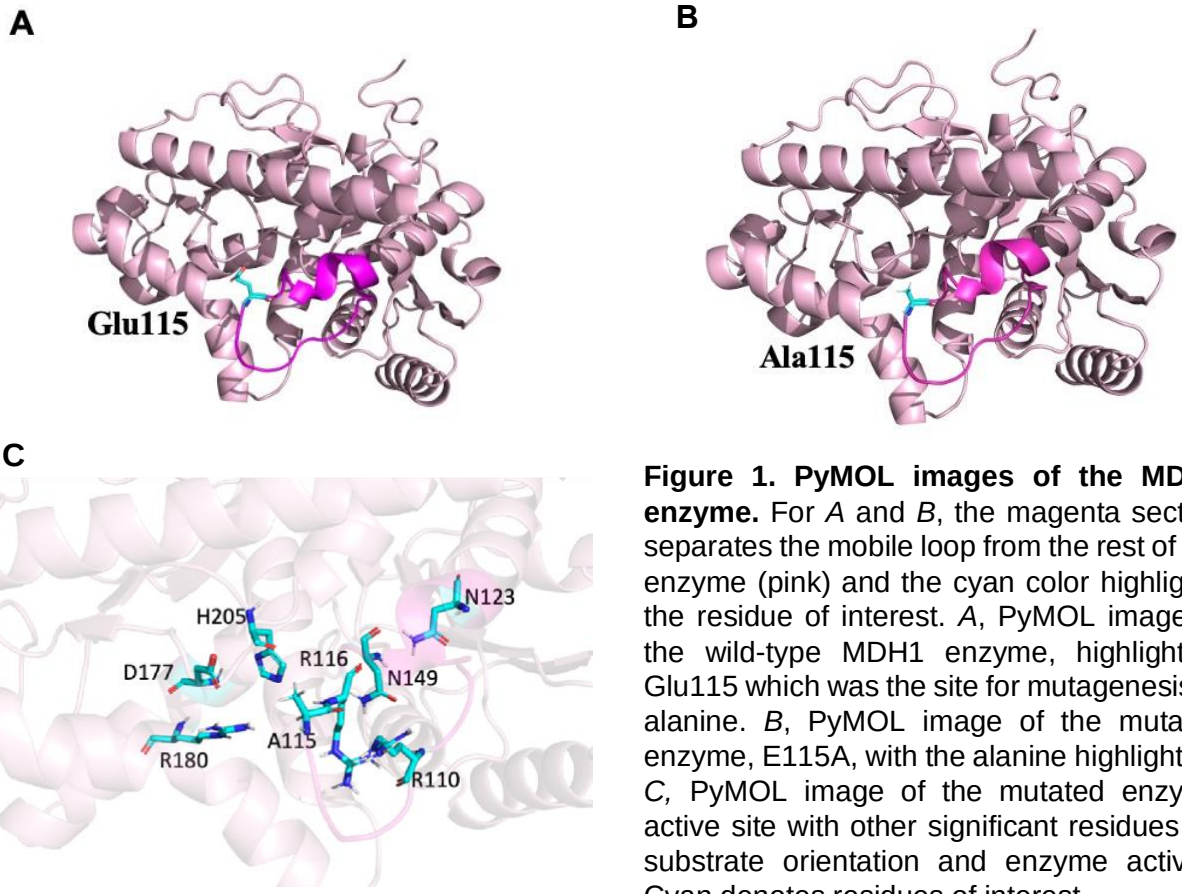

Figure 1. PyMOL images of the MDH1 enzyme. For *A* and *B*, the magenta section separates the mobile loop from the rest of the enzyme (pink) and the cyan color highlights the residue of interest. *A*, PyMOL image of the wild-type MDH1 enzyme, highlighting Glu115 which was the site for mutagenesis to alanine. *B*, PyMOL image of the mutated enzyme, E115A, with the alanine highlighted. *C,* PyMOL image of the mutated enzyme active site with other significant residues for substrate orientation and enzyme activity. Cyan denotes residues of interest.

then used to predict the docking of the substrate phenylpyruvate and to evaluate the energetics of the binding of the phenylpyruvate to the enzyme's active site using the programs SwissDock and Chimera (6,7). The SwissDock and Chimera data were used to identify the closest phenylpyruvate dockings to the active site and the free energy values were then calculated (Fig. 2). The average of the ΔG values was determined to be about -6 kJ/mol. The program H^{++} was then used to determine how the pK_a values of neighboring amino acid side chains are impacted by the E115A mutation (8). The mutation was found to affect the catalytic dyad residues the most significantly (His205 and Asp177) (Fig. 3).

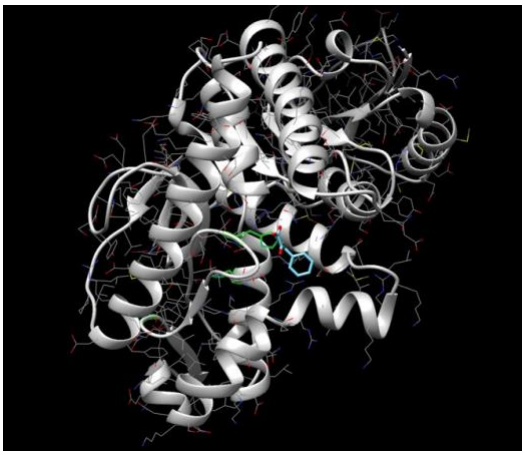

Figure 2. Chimera docking images of phenylpyruvate in mutant MDH1 enzyme. The Chimera results from the SwissDock data provided for the docking of phenylpyruvate in the active site of the MDH1 enzyme. Highlighted is the histidine 205 in the active site and the cyan-colored molecule is the phenylpyruvate.

Extraction of wild-type plasmid DNA

The isolated plasmid DNA quality was assessed by Nanodrop spectroscopy (9). The DNA of the wild-type plasmid from the *E. coli* cells expressing the MDH1 enzyme was determined to have a concentration of 1220 ng/µL. The 260/280 ratio was 2.22. The 260/230 ratio was 2.74 (Fig. 4).

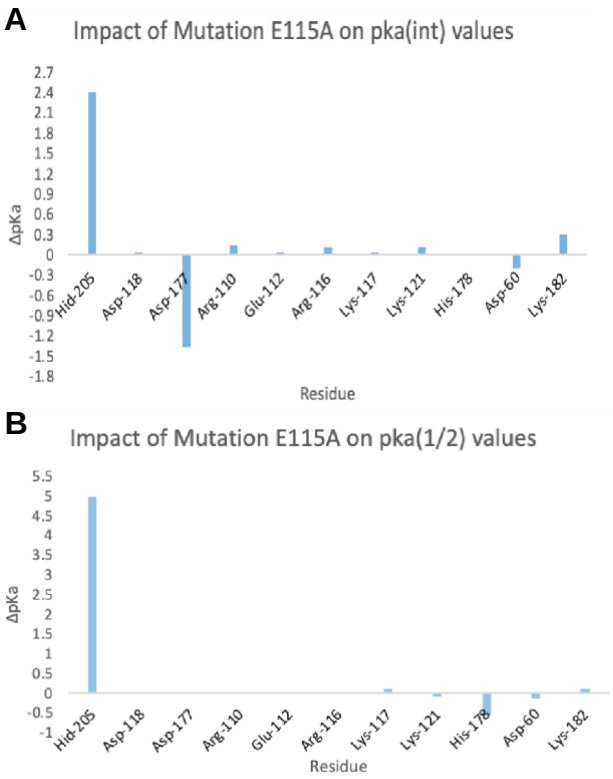

Figure 3. H^{++} analysis of E115A mutation impact on p*K*a values of neighboring amino acid side chains. *A,* The impact of E115A mutation on pK_a (int) values. *B,* The impact of E115A mutation on pK_a (1/2) values. ΔpK_a = mutant – wild-type.

Restriction digest analysis of wildtype MDH1 plasmid DNA

The wild-type plasmid was then assessed with a restriction digest to confirm that the plasmid was extracted and isolated. Restriction enzymes XhoI and NcoI were used to cut the enzyme and Figure 5*A* displays the virtual digest which shows bands at 5000 bp, 800 bp, and 200 bp. Experimentally, a band was seen at a size of 5000 bp, a potential band is seen at a size of 800 bp, and the gel smears too much at the bottom to see any smaller bands (Fig 5*B*).

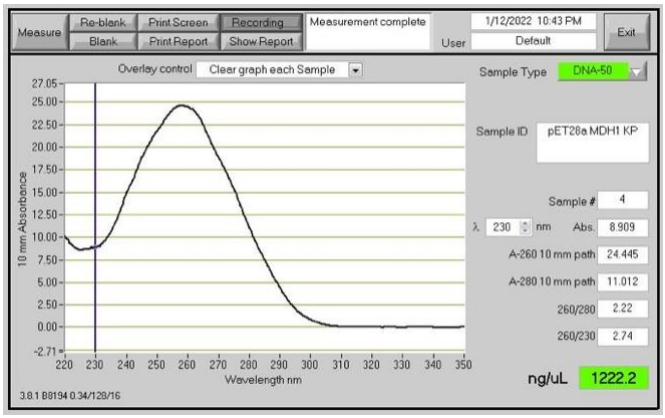

Figure 4. Nanodrop of wild-type plasmid. Nanodrop results of the DNA from the wild-type MDH1 variant 1 enzyme.

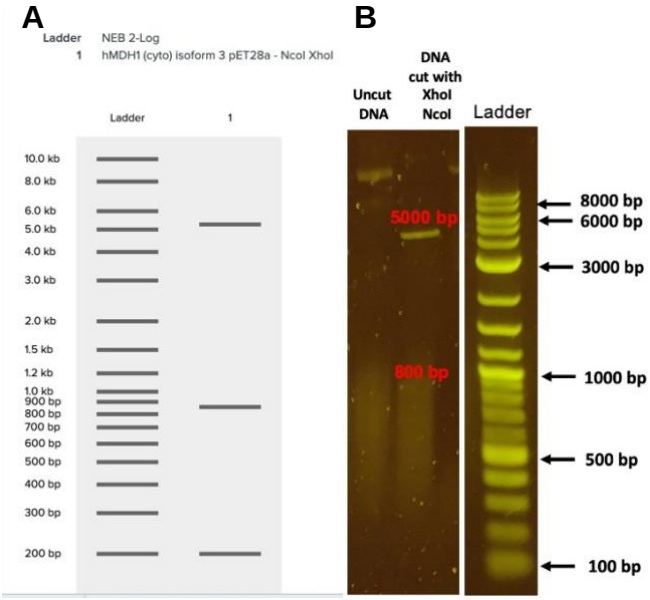

Figure 5. *A,* Virtual digest of wild-type MDH1 variant 1 with enzymes NcoI and XhoI. *B,* Electrophoresis gel of restriction digest of wild-type MDH1 variant 1 enzyme DNA with enzymes NcoI and XhoI.

Site-directed mutagenesis to introduce the E115A mutation

The E115A mutation was constructed in the MDH1 pET28a plasmid through site directed mutagenesis. Gel electrophoresis showed a band about 6000-7000 bp compared to the ladder (Fig. 6). The Nanodrop spectrophotometer then displayed a mutant DNA concentration of 48.9 ng/µL, a 260/280 ratio of 1.70, and a 260/230 ratio of 1.90 (Fig. 7).

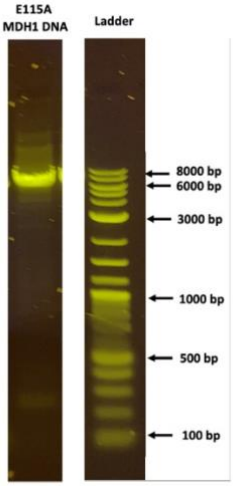

Figure 6. Site directed mutagenesis gel. PCR results of the site-directed mutagenesis to mutate the glutamate at position 115 of the MDH1 enzyme to an alanine.

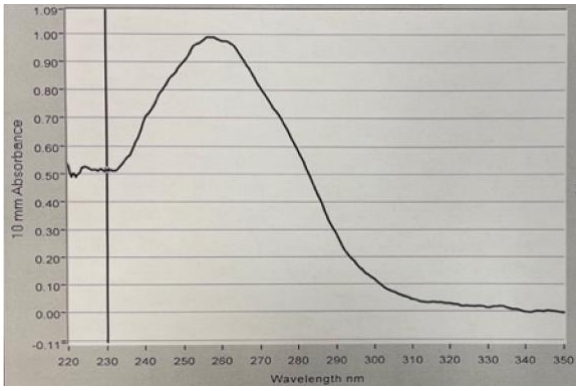

Figure 7. Site directed mutagenesis Nanodrop. Results from the Nanodrop of the purified mutant plasmid DNA containing the E115A mutation.

Mutant plasmid DNA sequencing results

The mutant plasmid was sent for sequencing by GeneWiz, and the results were analyzed with Benchling by aligning the mutant sequence with the wild-type sequence. The alignment has one difference between the mutant and wild-type DNA in the codon at position 115 (Fig. 8).

Figure 8. Alignment of the sequencing results of the site-directed mutagenesis DNA by GeneWiz with the wild-type sequence analyzed through Benchling. This alignment shows the residues near the 115 position where the mutation of glutamate (encoded by GAG) to alanine (GCG) was made.

Figure 9. Transformation of MDH1 E115A mutant into NEBα cells. The plate shows the transformation of the pET28a cells expressing the E115A mutation into *E. coli* NEBα cells.

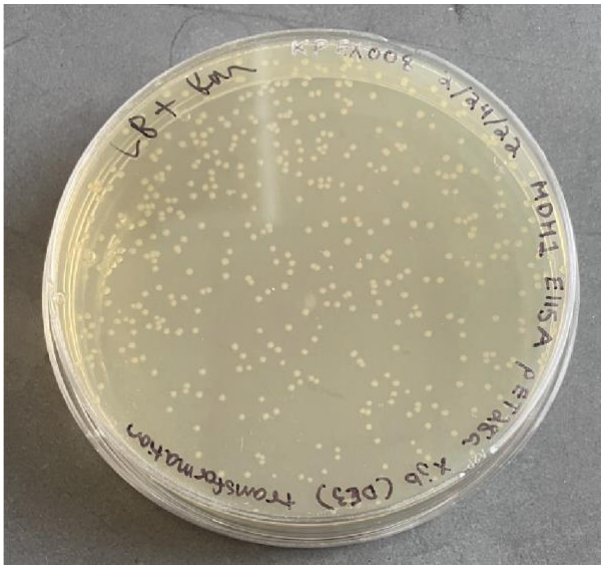

Figure 10. Transformation of MDH1 E115A mutant into XJb (DE3) cells. The plate shows the transformation of the pET28a cells expressing the E115A mutation into *E. coli* XJb (DE3) cells.

Transformation of E115A mutant cells

The mutant plasmid DNA was transformed into *E. coli* BL21 (DE3) NEBα cells and transformants were seen when plated (Fig. 9). The plasmid DNA from these cells was then isolated and transformed into *E. coli* XJb (DE3) cells. Transformants were seen (Fig. 10). The transformation efficiency of the transformed XJb (DE3) cells was 4.75 x 10^3 transformants/µg.

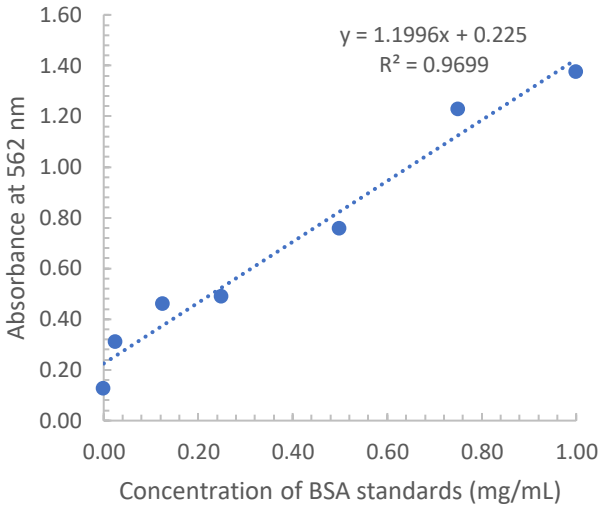

Figure 11. Standard curve of BCA assay. The figure shows the plot of concentration of the standards versus their absorbance with line equation shown.

Protein assays of purified protein

The mutant protein was purified by Ni-NTA chromatography, and the concentration was determined using a bicinchoninic acid (BCA) assay (10). A standard curve was plotted using several BCA standards and the slope was then used to determine the concentration of the protein, which was 0.75 ± 0.03 mg/mL (Fig. 11). SDS-PAGE analysis was then used to determine the molecular weight of the mutated protein (Fig. 12*A*). The log of the distance traveled by the standards in the ladder was plotted against the square

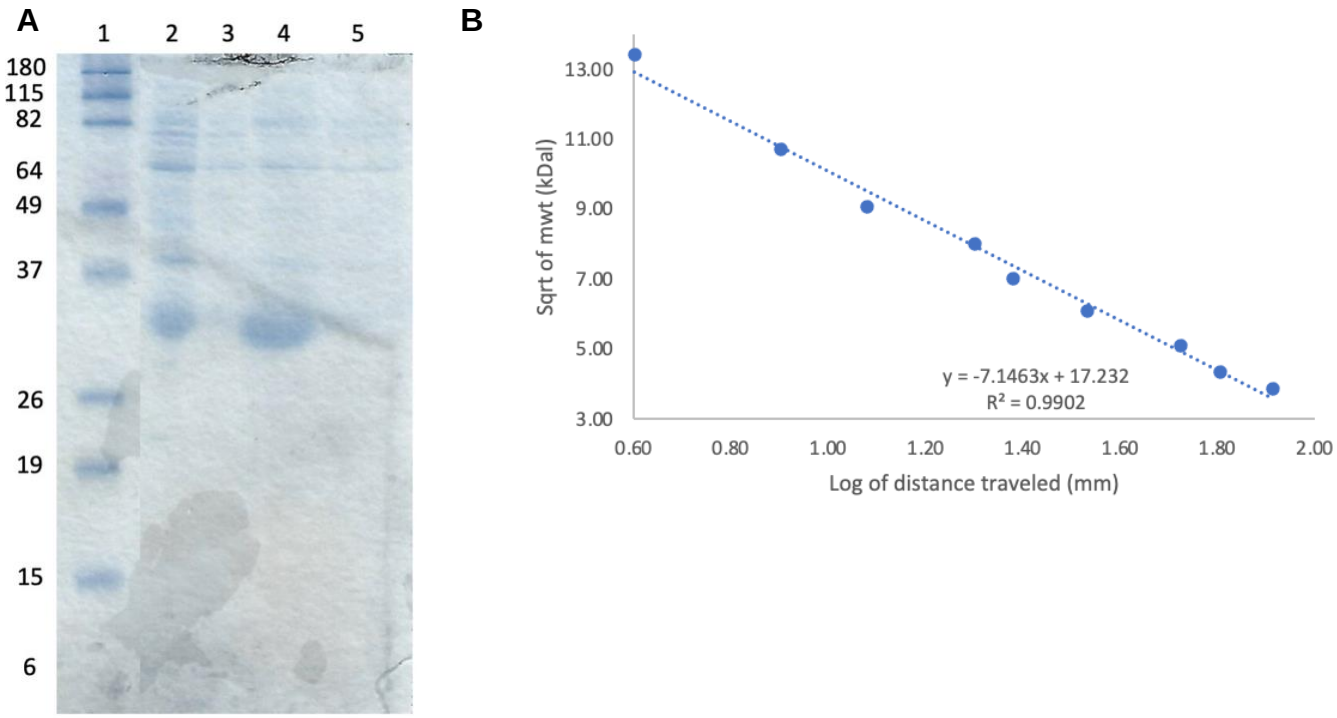

Figure 12. SDS-PAGE analysis of E115A MDH1 mutant protein. *A,* Lane 1 contains the ladder, lane 2 contains the cell lysate, 3 contains the flow through, 4 contains the mutant E115A protein, and lane 5 contains the wash. *B,* Standard curve of the log of the distance traveled by the ladder versus the square root of the molecular weight of the standards in the ladder.

root of the molecular weights of the standards and the slope of the line was then used to determine the molecular weight of the mutant protein. The protein was determined to be 33 kDa (Fig. 12*B*).

Kinetics assay of wild-type and mutant enzyme on OAA and phenylpyruvate

The activity of the wild-type and mutant enzymes on OAA and phenylpyruvate were then analyzed through kinetics analysis. Figure 13*A-D* displays the observed rate constants (k_{obs}) versus the concentrations of the substrate in the assay. The curve was then used through Wolfram Mathematica to determine the kinetic constants of the wildtype and mutant enzymes (Table 1).

Discussion

To contribute to the study of the human cytosolic malate dehydrogenase enzyme, the effect of the mutation of glutamate at position 115 to an alanine on activity and substrate specificity was assessed. This mutation was believed to introduce a neutral, hydrophobic residue into the mobile loop which would change the specificity and activity of the enzyme, potentially making it more active on phenylpyruvate. Phenylpyruvate is larger than OAA and more nonpolar, so changing some of the qualities of the mobile loop and how the enzyme folds may allow the active site to accommodate a larger substrate. The programs AlphaFold, Chimera, and H^{++} were utilized to predict that the mutation would

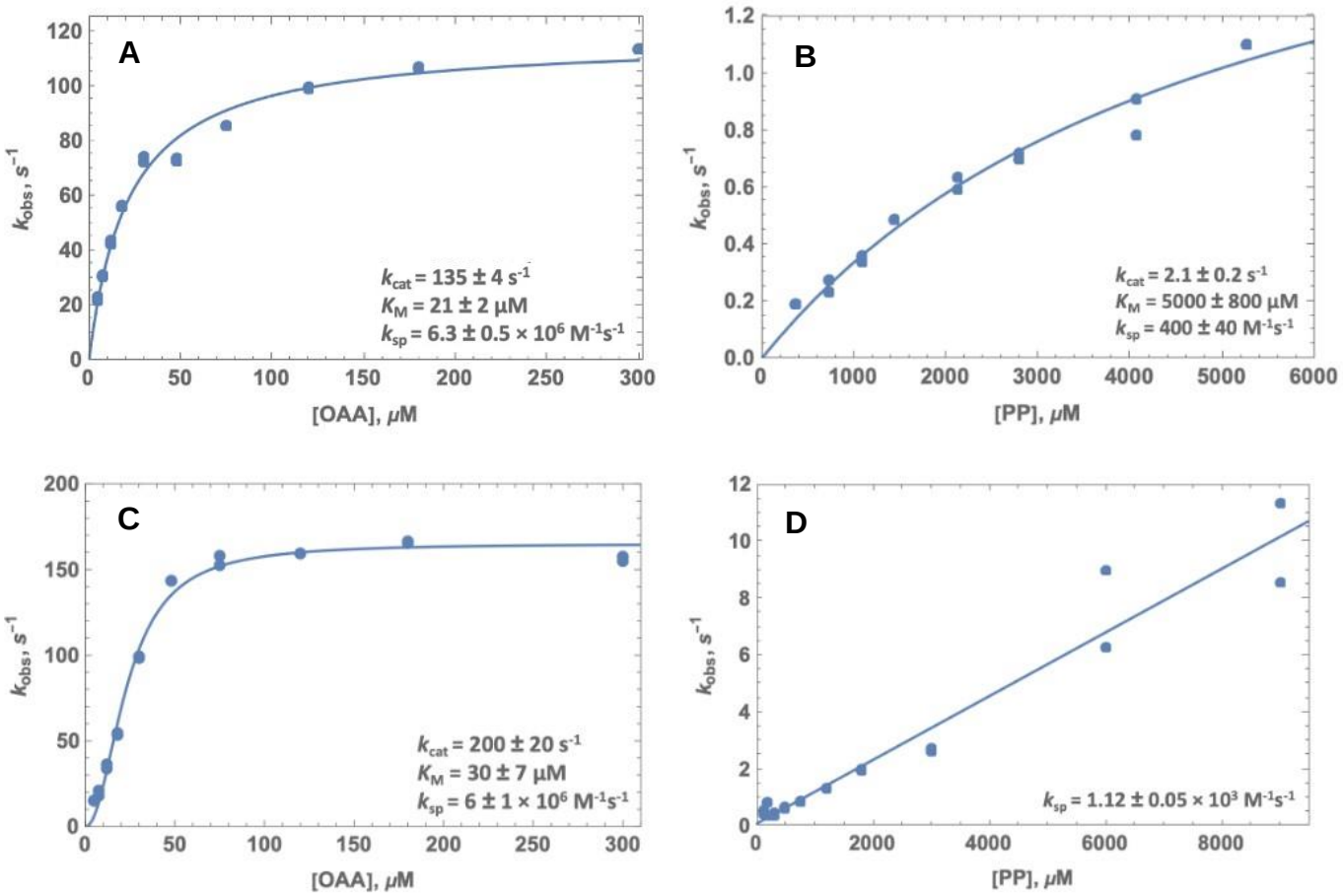

Figure 13. Kinetics assay of MDH1 E115A mutation and wild-type on OAA and phenylpyruvate. These curves show the data measuring the changes in absorbance of the solutions as NADH is oxidized to form NAD^+ in terms of k_{obs} versus concentration of substrate. *A,* The curve shows the analysis of E115A on OAA. *B,* Analysis of E115A on phenylpyruvate. *C,* Analysis of wild-type on OAA. *D,* Analysis of wild-type on phenylpyruvate.

Table 1
Enzyme kinetics assay of wild-type and E115A mutant on OAA and phenylpyruvate data.

Substrate	OAA		Phenylpyruvate	
MDH1 Enzyme	WT	E115A	WT	E115A
k_{cat} (s^{-1})	200 ± 20	135 ± 4	Undefined	2.1 ± 0.3
K_M (µM)	30 ± 7	21 ± 2	>9000 µM	5100 ± 800
k_{sp} ($M^{-1}s^{-1}$)	6 ± 1 × 10^6	6.3 ± 0.5 × 10^6	1.12 ± 0.05 × 10^3	400 ± 40

affect a few neighboring amino acids and in turn change the enzyme's activity (Fig. 2,3). The H^{++} results predicted that the mutation would mostly affect the His205 and Asp177 which are part of the catalytic dyad. This would mean that the mutation potentially changes the activity and thus the efficiency of the enzyme. The wild-type of the MDH1 protein was prepared through a plasmid miniprep of liquid cultures using a kit from Zymo Research (11). The wild-type DNA had a substantial concentration of 1220 ng/µL.

The 260/280 ratio was close to the range of 1.8-2.0 which indicates purity of the DNA, suggesting that the wild-type DNA was relatively pure and may only have slight contamination of RNA in the sample. The 260/230 ratio was slightly higher than the optimal range of 2.0-2.2. The restriction digest ensured the presence of the DNA with the gel demonstrating that the correct cut was made by the XhoI enzyme at about 5000 bp, but the smearing of the gel makes it difficult to determine if the correct cuts were made that would result in bands at sizes 861 bp and 200 bp. While the presence of the other two bands was unclear, the cut resulting in an estimated 5000 bp sized band suggests that the wild-type plasmid was present.

The success of the site-directed mutagenesis to implement the E115A mutation in the MDH1 pET28a plasmid was confirmed through gel electrophoresis as bands were seen between 6000 and 7000 bp when the actual size is 6292 bp (Fig. 6). The concentration was 48.9 ng/µL and the 260/280 and the 260/230 ratios were close to purity. The presence of the mutation was then further confirmed by the sequencing of the plasmid DNA by GeneWiz. Figure 8 shows the alignment of the sequencing results with the wild-type plasmid sequence near the 115 position where the mutation was made. The change from the GAG codon which codes for glutamate to GCG which codes for alanine indicates that the mutation was made successfully.

The E115A mutant plasmid DNA overexpression and transformation into *E. coli* XJb (DE3) cells was successful, but the transformation efficiency was 4.75 x 10^3 transformants/µg which is lower than the expected efficiency of 10^8 transformants/µg. Ni-NTA chromatography purified the E115A mutant MDH1 protein with 250 mM imidazole PBS elution (12). The mutant protein was determined to have a concentration of 0.75 ± 0.03 mg/mL (10). SDS-PAGE analysis determined the molecular weight of the E115A mutated MDH1 protein to be 33 kDa which is relatively close to, but smaller than, the estimated molecular weight of 39.7 kDa (Fig. 12).

The activity of the purified protein was then analyzed on its native and non-native substrates through various kinetics assays. The kinetic constants of the wild-type and mutated enzymes are reported in table 1. The k_{cat} values for wild-type and E115A enzymes on OAA were 200 ± 20 s^{-1} and 135 ± 4 s^{-1} respectively (Table 1). This suggests that the enzyme's turnover rate efficiency of OAA was decreased by the mutation at position 115. The K_M value for the wild-type enzyme (30 ± 7 µM) was higher than that of the E115A enzyme (21 ± 2 µM) on OAA, suggesting that the mutation slightly increased the enzyme's affinity for OAA, since a smaller K_M value indicates a higher affinity. The k_{sp} value for the mutant enzyme, $6.3 \pm 0.5 \times 10^6$ $M^{-1}s^{-1}$ was almost identical to the wild-type k_{sp} of $6 \pm 1 \times 10^6$ $M^{-1}s^{-1}$. k_{sp} is a measure of an enzyme's specificity for a given substrate, so the mutant enzyme has the same specificity as the wild-type for OAA. The wild-type OAA data fit to a sigmoidal curve better than hyperbolic, indicating cooperativity. The Hill coefficient, *n*, was calculated to be 2 and when $n > 1$ it is an indication of cooperativity. More trials will need to be conducted to confirm this observation, as MDH enzymes are not believed to have cooperative binding. The phenylpyruvate data for the wild-type enzyme

do not conform to a hyperbolic curve, so a value can only be reported for the k_{sp}. The k_{sp} was determined from the linear fit of the data and is from the slope of the line. The wild-type enzyme had a k_{sp} of $1.12 \pm 0.05 \times 10^3$ $M^{-1}s^{-1}$ and the mutant enzyme had a k_{sp} of $0.40 \pm 0.04 \times 10^3$ $M^{-1}s^{-1}$. The higher k_{sp} of the wildtype enzyme than the mutant for phenylpyruvate suggests that the mutation resulted in a lower specificity of the enzyme for phenylpyruvate. The mutation was also much less specific for phenylpyruvate than it was for OAA. This means that the E115A mutation of the MDH1 enzyme did not make the enzyme more accommodating to the nonnative substrate, phenylpyruvate, over OAA. The mutant enzyme's higher k_{sp} for OAA than phenylpyruvate suggests that the enzyme still prefers OAA, the native substrate, over the non-native substrate. The mobile loop of the enzyme folds over the active site when the enzyme-coenzymesubstrate complex forms and this conformational change screens the substrate and important residues from the solvent. This brings the catalytically important residues closer to the substrate (13). It was believed that the mutation of glutamate to a smaller, hydrophobic residue would alter the conformational change of the mobile loop and allow for phenylpyruvate to bind more preferably. However, the lower specificity of the mutant for phenylpyruvate than for OAA does not support this proposal.

The mutant enzyme also had a much lower k_{cat} and much higher K_M value for phenylpyruvate than for OAA, suggesting that the mutation made the enzyme less efficient at turning over product from phenylpyruvate because of a lower affinity for phenylpyruvate than for OAA. This is because the enzyme required a higher concentration of phenylpyruvate to turn over product. It was believed that the substitution of alanine for glutamate would result in a higher affinity for phenylpyruvate as a substrate because it was smaller and would allow for the larger substrate to fit in the mobile loop during its conformational change, however, this did not appear to occur.

The data from the wild-type OAA kinetics assay is somewhat different from the data presented in other literature. In the paper by Wright et. al, the k_{cat} for wild-type MDH1 on OAA is reported to be 780 ± 125 s^{-1} which is much larger than our reported k_{cat} value for wild-type MDH1 on OAA which was 200 ± 20 s^{-1} (14). The literature k_{sp} value for wildtype MDH1 for OAA was 1.9×10^7 $M^{-1}s^{-1}$ which is much higher than what we reported as a value of $6 \pm 1 \times 10^6$ $M^{-1}s^{-1}$. For the wildtype MDH1 on phenylpyruvate, the k_{sp} was 8.7×10^3 $M^{-1}s^{-1}$ which is to the same order of magnitude as our reported k_{sp} for the wildtype enzyme on the same substrate. More assays may need to be completed to find an agreement between our values and those of other literature.

Overall, we report that the mutation of glutamate at position 115 to alanine significantly changed the enzyme's affinity and specificity for OAA and phenylpyruvate. This mutation was predicted to make the enzyme more efficient for the binding of phenylpyruvate, however the kinetics data suggest that it instead led to a higher affinity for the native substrate and a lower affinity for the non-native substrate as well as a decreased specificity for both substrates compared to the wild-type.

Further research in this area would include more assays of the wild-type enzyme on

phenylpyruvate to be able to report the k_{cat} and K_M. Fitting the data to a hyperbolic curve will allow for comparison to the mutant assay kinetics values. Further investigation of the kinetics data can be conducted to confirm the accuracy of the assays. Further research can also be conducted with other substrates and mutations of the enzyme to determine optimal kinetic conditions of the enzyme. As further results are concluded, the opportunity can arise to manipulate the affinity of the enzyme to a non-native substrate that might inhibit the enzyme in cancer cells.

Experimental procedures

Preparing liquid cultures of BL21 (DE3) pET28a MDH1

For inoculating an overnight liquid culture for plasmid miniprep, a single colony was used from a bacterial Luria-Bertani (1% tryptone, 0.5% yeast extract, 1% NaCl, 3% agar, pH 7) medium + 50 µg/mL kanamycin plate of BL21 (DE3) cells with pET28a plasmid expressing the MDH1 gene. A colony was scraped from the agar plate and rubbed off into LB + 50 µg/mL kanamycin medium. The culture was then grown overnight at 28˚C with shaking at 250 rpm. The culture was then centrifuged, the supernatant was discarded, and the pellet was used for a plasmid miniprep.

Plasmid miniprep of BL21 (DE3) pET28a MDH1

To extract the plasmid expressing the MDH1 gene from a culture of *E. coli* cells, a Zyppy Plasmid miniprep kit from Zymo Research, Tustin, California was used. Liquid overnight cultures were prepared prior to the miniprep and contained pET28a plasmid containing the MDH1 gene. A slight adaptation from the manufacturer recommended protocol was followed. The 3 mL bacterial culture was pelleted and frozen prior to starting the plasmid miniprep, then thawed and resuspended in TE buffer (10 mM Tris and 1 mM EDTA). After the neutralization step, multiple cycles of centrifugation were carried out to fully separate the supernatant and the precipitate. Before the elution step, an optional step was carried out by washing the column with 95% ethanol by centrifuging at 16,000 × g for 30 seconds. The DNA was eluted with prewarmed Zyppy Elution Buffer (10 mM Tris, 0.1 mM EDTA, pH 8.5, 50˚C). Once the DNA was collected, the Nanodrop spectrophotometer was then used to measure the absorbance of the plasmid DNA at 260 nm and 280 nm to assess the DNA purity.

Restriction digest of pET28a MDH1

For a double restriction digest, a reaction containing CutSmart NEB Buffer, 1 µg of DNA purified from the plasmid miniprep, 10 units each of NcoI and XhoI restriction enzymes from New England BioLabs (NEB) were combined. A separate reaction without the restriction enzymes was prepared. The samples were incubated at 37˚C for 15 minutes. A 1% agarose gel was prepared by dissolving agarose in TBE (89 mM Tris, 89 mM boric acid, 2 mM EDTA). SybrSafe was added directly to the gel. NEB QuickLoad 1 kb plus ladder was used and 30 µL of each sample was combined with 5 µL of 6X loading dye. The gel was run at 80V for 1 hour and 40 minutes and was shaken in a staining solution of 10 µL of SybrSafe in 100 mL of water, then placed on the shaker for 15

minutes for better visualization on the Dark Reader Transilluminator.

Multiple Sequence Alignment

To determine which mutation to carry out in the malate dehydrogenase enzyme, first a multiple sequence alignment (MSA) was carried out. The MSA was conducted using UniProt (3) by searching for malate dehydrogenase 1 (UniProt ID code: P40925) and filtering by different classes that contained the enzyme in the cytoplasm. A range of organisms was found and added to the basket, and then the alignment was made. Once the alignment was completed, a list was compiled of the residues that were conserved in each organism (indicated by an asterisk under the alignment). These conserved residues are immutable and thus were removed from the potential residues that were chosen from for the single-point mutation. The mutation residue choice was also limited to the mobile loop on the enzyme, which is between residues 105 through 123. Glu115 is within the mobile loop, and is mutable, so it was chosen to be mutated. Referring to the MSA, the residue at 115 was occasionally a threonine or an aspartate instead of glutamate, so these residues were not chosen for the mutation. Instead, alanine was chosen because it would result in a change in size, charge, and hydrophilicity. Benchling was used to acquire the DNA sequence of the MDH1 enzyme, and the sequence was input into NEBaseChanger from NEB labs to design the primers. The wild-type sequence GAG was mutated to GCG to code for alanine and the primers were automatically designed. The primers were then ordered from Integrated DNA Technologies, Coralville, IA.

Site-Directed Mutagenesis

Primers were ordered from Integrated DNA Technologies, Coralville, IA, and the New England BioLabs Q5 site-directed mutagenesis kit and protocol was used (catalog number E0554). The sequence of the forward primer was 5'…GAAGGCATGGCGAGAAAAGATTTACTG…3' and the reverse primer sequence was 5'…CCTTCTTGGAGCC…3'. For exponential amplification by PCR, a PCR mixture was then assembled containing Q5 Hot Start high-fidelity Master Mix, the 0.5 µM forward primer, the 0.5 µM reverse primer, 25 ng of the template DNA from the plasmid miniprep, with a final volume of 25 µL. The thermocycler was programmed for PCR. The initial denaturation was at 98˚C for 30 seconds, then there were 30 cycles consisting of 10 seconds of denaturation at 98˚C, 30 seconds of annealing at 63˚C, extension for 2 minutes and 30 seconds at 72˚C, and final extension for 2 minutes at 72˚C. A 1% agarose gel was prepared in TBE. SybrSafe was added directly to the gel. NEB QuickLoad 1 kb plus ladder was used and 10 µL of the PCR mixture was diluted with blue loading dye (NEB), and electrophoresis was run for one hour at 80V. For kinase, ligase, and DpnI (KLD) treatment, a mixture was assembled containing the PCR product, 5 µL of 2X KLD reaction buffer, and 1 µL of 10X KLD enzyme mix to a final volume of 10 µL. The mixture was then incubated for 5 minutes. For the transformation, NEB 5a competent *E. coli* cells were thawed on ice, and 5 µL of the prepared KLD mixture was added and mixed with the cells. The mixture was placed on ice for 30 minutes, heat shocked at 42˚C for 30 seconds, and then placed on ice for 5 minutes. To this, 950 µL

of room temperature SOC media was added, and the mixture was then incubated at 37˚C for one hour shaking at 180 rpm. The cells were mixed thoroughly and 100 µL of the cell mixture was plated on one prewarmed Luria-Bertani medium + 50 µg/mL kanamycin plate. The rest of the mixture was centrifuged at 3000 × g for 3 minutes, the top 900 µL was removed, then the remaining 100 µL was used to resuspend the pellet and plated on another prewarmed Luria-Bertani medium + 50 µg/mL kanamycin plate. The plates were incubated overnight at 37˚C for transformants to grow.

Preparing liquid cultures of NEB5α pET28a mutant E115A MDH1

Liquid cultures were prepared as explained above, using a bacterial plate of BL21 (DE3) cells with pET28a plasmid expressing the MDH1 gene with the E115A mutation.

Plasmid miniprep of NEB5α pET28a MDH1 with E115A mutation

To extract the MDH1 gene expressing plasmid DNA from the cultures of *E. coli* cells, a Zyppy Plasmid miniprep kit from Zymo Research, Tustin, CA was used as explained above. The elution step varied in that 10 mM Tris (pH 7.5) warmed to 50˚C was used. Once the DNA was collected, the Nanodrop spectrophotometer was then used to measure the absorbance of the plasmid DNA at 260 nm and 280 nm.

Sample preparation for DNA sequencing

The mutant colony samples were prepared according to GeneWiz and the plasmid DNA was sent for sequencing by GeneWiz to ensure that the E115A mutation was present in each plasmid DNA. T7 primers were used for sequencing.

Bacterial transformation and protein overexpression

For bacterial transformation of the mutant protein, Z-competent XJb (DE3) Autolysis Mix & Go cells from Zymo were used to take up the mutant plasmid. The mutant DNA (100 ng) DNA was mixed with 50 µL of the XJb (DE3) cells. The cells were incubated on ice for ten minutes. To the cells, 4 volumes of SOC media were added and then the cells were incubated for one hour at 37˚C with gentle shaking in the water bath. A prewarmed agar plate containing LuriaBertani medium + 50 µg/mL kanamycin was used for plating the transformations. Before plating, the cells were spun down at 3,000 × g for 3 minutes. The supernatant was taken off so that there was only 100 µL of sample left to plate, which was then plated. The plates were then incubated overnight at 37˚C, for no more than 18 hours to prevent satellite colony formation. The plates were then parafilmed and stored at 4˚C.

Preparing liquid cultures of XJb (DE3) pET28a mutant E115A MDH1

Liquid overnight cultures were prepared as explained above, using a bacterial plate of XJb (DE3) cells with pET28a plasmid expressing the MDH1 gene with the E115A mutation. The overnight culture was then used to start a 50 mL expansion culture with a starting OD of 0.05 in Luria-Bertani medium + 50 µg/mL kanamycin. The culture was then incubated at 37˚C with periodic OD measurements until the absorbance was about 0.55-0.6. The culture was then cooled in an ice water bath to room temperature. The

cultures were induced by adding IPTG to a final concentration of 0.5 mM. Arabinose was then added to a final concentration of 3 mM. The cells were then grown overnight at 20˚C at 250 rpm.

Cell lysis of E115A MDH1 protein

To lyse and purify the XJb (DE3) cells overexpressing the E115A mutation, freezethaw cycles essential for lysis were carried out. First, the cells were harvested by centrifugation at 3000 × g for 10 minutes at 4˚C and resuspended in 3 mL of lysis buffer (20 mM Tris, 100 mM NaCl, pH 8.0) with a Pierce protease inhibitor tablet (product #A32955, 1 tablet per 10 mL lysis buffer). The resuspended pellet was then frozen and thawed. A second freeze/thaw cycle was carried out using liquid nitrogen. The sample was then mixed with 0.02 U/µL DNAse I and 1 mg/mL lysozyme. The mixture was then shaken at 250 rpm for 30 minutes at 37˚C, and then centrifuged at 15,000 × g for 30 minutes at 4˚C. The pellet was then discarded, and the supernatant was saved.

Ni-NTA affinity chromatography

To purify the desired protein using nickel affinity chromatography (2), a 4 mL slurry of Thermo Scientific HisPur Ni-NTA resin (Catalog #88221) was used. The cell lysate sample from the cell lysis procedure and the Ni-NTA resin were combined and mixed on an end-over-end rotator for 30 minutes at 4˚C. The mixture was then spun down for 1 minute at < 800 × g, the supernatant was taken off and saved, then PBS (20 mM sodium phosphate, 300 mM sodium chloride, pH 7.4) was used to resuspend the resin. The slurry was then placed in a glass column and the flow through was collected. The resin was then washed with about 20 bed volumes of PBS with 10 mM imidazole until the measured absorbance was about 0.1. The protein was then eluted with about 4 bed volumes of PBS containing 250 mM imidazole and the absorbance was measured. The eluant was then placed in Spectra/Por 1 dialysis tubing and put into 3.5 L of PBS buffer with stirring at 4˚C and the buffer was replaced two times.

BCA assay of MDH1 E115A protein

To determine the concentration of the desired protein, a bicinchoninic acid (BCA) assay was performed (3). A series of diluted BSA (Pierce, Product #23209) standards were then prepared in a range from 0 to 1.500 mg/mL for the assay. A working reagent was then prepared by combining reagent A (containing Na_2CO_3, $NaHCO_3$, BCA and sodium tartrate in 0.1 M NaOH) and reagent B (4% $CuSO_4 \cdot 5\ H_2O$) from Pierce (Product #23225) in a 50:1 mL ratio and 1 mL of the working reagent was then added to each standard as well as to samples of the protein with unknown concentration. The 50 µL samples were then placed in a water bath at 37˚C for 20 minutes with shaking at 100 rpm. The absorbance of each sample was then measured at 562 nm.

SDS-PAGE large gel of MDH1 E115A protein

SDS-PAGE was carried out using the method of Laemmli (15) apart from the sample buffer containing 2 mM DTT in each sample and 1% β-mercaptoethanol. The gel was run at 55 mA through the 3% acrylamide stacking gel and 30 mA through the 12.5% acrylamide separating gel. The gel was removed from the plate and placed in

Coomassie Blue stain staining solution (0.025% Coomassie Blue R-250, 40% methanol, 7% acetic acid), shaken overnight at 80 rpm, and the stain solution was replaced until the gel was clear. The gel was then placed in destaining solution (40% methanol, 7% acetic acid, 3% glycerol) and shaken at 80 rpm until destained. To dry, the gel was placed in a solution of 7% methanol and 3% glycerol and was then placed on the gel dryer under vacuum for 2 hours at 80˚C and then for one hour at room temperature.

Kinetics assay of MDH1 E115A protein on oxaloacetate and phenylpyruvate

Kinetic constants were determined through a kinetics assay of the malate dehydrogenase mutant on oxaloacetate (OAA) and phenylpyruvate with NADH as a cofactor. Measurements of the absorbance changes due to the disappearance of NADH were taken in duplicate at 340 nm over the course of 30 seconds. The working solution was in 3000 µL of 100 mM potassium phosphate assay buffer with 0.11 mg/mL NADH (pH 7.4). The enzyme concentration in the assay was 8.25 nM. For the OAA trials, OAA was added in varying concentrations ranging from 4.8 µM to 300 µM. For the phenylpyruvate trials, concentrations ranging from 370 µM to 5300 µM were used in the working solution. The slope of each of the absorbance versus time curves (AU/minute) were converted to the observed rate constant (k_{obs}) by converting the slope to nM/second using the concentration of the enzyme in the assay and then dividing by the molar coextinction coefficient (ε) of NADH which was 0.006220 $\mu M^{-1}cm^{-1}$. The k_{obs} was then plotted against the concentration of the substrate in the assay and the kinetics constants were then obtained from this data using a Mathematica program and a modified Michaelis-Menten equation to fit the data (16):

$$v = \frac{k_{sp}[S]}{1 + k_{sp}/k_{cat}}$$

Where $k_{sp} = k_{cat}/K_M$ and represents the enzyme's specificity and efficiency, v is the velocity, and [S] is the substrate concentration. The kinetic constants k_{cat}, K_M, and k_{sp} were calculated for wild-type enzyme and the E115A mutant enzyme on OAA and phenylpyruvate.

Acknowledgements—We thank the Department of Chemistry and Biochemistry, particularly the department chair, Dr. Kenneth Overly. We thank the Biology Department, namely Dr. Brett Pellock for providing support for this course. We thank the members of the CHM 310L course. We appreciate the New England BioLabs for providing the restriction enzymes as a gift. We acknowledge the MDH CURE Community (MCC) for their invitation of Providence College to join the program. Additionally, we thank Dr. Jessica Bell, University of San Diego, for providing the *E. coli* BL21 (DE3) cells containing the MDH1 expressing pET28a plasmids. Lastly, we thank Dr. Joseph Provost, University of San Diego, for constructing the MDH models.

References

1. Abtahi, N., S., Shahriari, A., Talaiezadeh, A., and Fathizadeh, P. (2017) Kinetic characterization of malate dehydrogenase

in normal and malignant breast tissues. *Biomed Res.* **28,** 4329-4344
2. Mansouri, S., Shahriari, A., Kalantar, H., Zanjani, T. M., and Karamallah, M. H. (2017) Role of malate dehydrogenase in facilitating lactate dehydrogenase to support the glycolysis pathway in tumors. *Biomedical Rep.* **6**, 463-467
3. The UniProt Consortium (2020) UniProt: the universal protein knowledgebase in 2021. *Nucleic Acids Res.* **49,** 480-489
4. The PyMOL Molecular Graphics System, Version 2.0 Schrödinger, LLC
5. Jumper, J., Evans, R., Pritzel, A., Green, T., Figurnov, M., Ronneberger, O., Tunyasuvunakool, K., Bates, R., Zidek, A., Potapenko, A., Bridgland, Meyer, C., Kohl, S. A. A., Ballard, A. J., Cowie, A., Romera-Peredes, B., Nikolov, S., Jain, R., Adler, J., Back, T., Peterson, S., Reiman, D., Clancy, E., Zielinski, M., Steinegger, Pacholska, M., Berghammer, T., Bodenstein, S., Silver, D., Vinyals, O., Senior, A. W., Kavukcuoglu, K., Kohli, P ., and Hassabis, D. (2021) Highly accurate protein structure prediction with AlphaFold. *Nature.* **596,** 583-592
6. Grosdidier, A., Zoete, and V., Michielin, O. (2011) SwissDock, a protein-small molecule docking web service based on EADock DSS. *Nucleic Acids Res.* **39,** 270-277
7. Pettersen E.F., Goddard, T. D., Huang, C. C., Couch, G. S., Greenblatt, D. M., Meng, E. C., and Ferrin, T. E. (2004) USCF Chimera—A visualization system for exploratory research and analysis. *J Comput Chem.* **25,** 1605-1612
8. Anandakrishnan, R., Aguilar, B., and Onufriev, A. (2012) H^{++} 3.0: automating pK prediction and the preparation of biomolecular structures for atomistic molecular modeling and simulations. *Nucleic Acids Res.* **40,** 537-541
9. Koetsier, G., and Cantor, E. (2019) A practical guide to analyzing nucleic acid concentration and purity with microvolume spectrophotometers. *New England BioLabs.* 1-8
10. Smith, P. K., Krohn, R. I., Hermanson, G. T., Mallia, A. K., Gertner, F. K., Provenzano, M. D., Fujimoto, E. K., Goeke, N. M., Olson, B. J., and Klenk, D. C. (1985) Measurement of protein using bicinchoninic acid. *Anal Biochem.* **150,** 76-85
11. Zymo Research (RRID:SCR_008968)
12. Block, H., Maertens, B., Spriestersbach, A., Brinker, N., Kubicek, J., Labahn, J., and Schafer, F. (2009) Immobilized-metal affinity chromatography (IMAC): a review. *Method Enzymol.* **463,** 439-473
13. Goward, C. R., and Nicholls, D. J. (1994) Malate dehydrogenase: a model for structure, evolution, and catalysis. *Protein Science.* **3,** 1883-1888
14. Wright, S. K., Kish, M. M., and Viola, R. E. (2000) From malate dehydrogenase to phenyllactate dehydrogenase. *J Biol Chem.* **275,** 31689-31694
15. Laemmli, U.K. (1970) Cleavage of structural proteins during the assembly of the head of bacteriophage T4. *Nature.* **227,** 680-685
16. Johnson, K. A. (2019) New standards for collecting and fitting steady state kinetic data. *J Org Chem.* **15,** 16-29